



OPEN

# Circular active noise barrier using theoretical control filter considering interaction between speaker and barrier

Sanghyeon Lee &amp; Youngjin Park

A circular active noise barrier using a theoretically calculated control filter without real-time adaptation was proposed for noise reduction in a specific outdoor space. A compact circular barrier is used for the movable system to cope with changes in the location of the workspace, and noise in a wide frequency band can be reduced by conducting active noise control through control speakers arranged around a barrier. However, there was a significant performance gap compared with the maximum performance achieved by using the experimental fixed filter due to an extremely simplified theoretical model which ignores the interaction between the control speakers and the barrier. Therefore, this study tried to minimize the performance degradation when applying the theoretically calculated control filter. Another theoretical model is introduced to improve the noise reduction performance by considering the interaction between the control speaker and the barrier. Through experiment, it is confirmed that noise reduction performance is improved by about 2.6 dB in the frequency of interest.

Noise problems in industrial settings are becoming more various and serious, and coupled with increasingly stricter noise regulations, noise reduction is becoming a more important issue. Noise in various spaces such as rest areas or workspaces can lead to stress, distraction, and hearing loss<sup>1</sup> and many workers in industries are exposed to loud noise for long periods of time. A noise barrier can be used to reduce noise, but it is ineffective for noise reduction in a low-frequency band due to the diffracted noise. In order to reinforce noise reduction in a low-frequency band, the active noise barrier<sup>2-6</sup> that applies active noise control (ANC)<sup>7</sup> to a barrier was studied. By placing speakers and error microphones above the barrier, the diffracted noise in a low-frequency band is reduced through ANC. The arrangement of microphones and speakers<sup>8,9</sup>, the method of obtaining the control filter<sup>10,11</sup>, and using unidirectional control sources<sup>12</sup> have been studied to improve the performance of the active noise barrier. However, the active noise barrier using semi-infinite barrier is expensive and requires a large place to set up. In addition, it is hard to move, so it is applicable only to a fixed environment.

In order to solve this problem, the circular active noise barrier using a theoretically calculated control filter<sup>13-15</sup> was proposed to reduce noise in a specific outdoor space instead of global noise reduction. The circular active noise barrier consists of a compact circular barrier and control speakers placed around the barrier with the aim of reducing noise in an individual target space such as a workspace or rest space. It requires less cost and space compared with the semi-infinite barrier, and can be moved and reinstalled. A theoretically calculated control filter without arranging microphones over the target space is used because the arranged microphones to apply ANC obstructs the workers. The theoretically calculated control filter can be calibrated quickly, so it is easy to respond to changes in the position of the noise source or the target control space.

However, the performance gap between the theoretically obtainable performance and the experimental results is significant. In the previous study<sup>13</sup>, a control filter is calculated based on an extremely simplified theoretical model aimed at providing a simply applicable noise control method. The performance degradation occurs due to the difference between the simplified theoretical model and the experimental system. Therefore, this study tried to minimize the performance degradation that occurs when the theoretically calculated control filter is applied to the circular hybrid noise control system. The interaction between the control speaker and the barrier, which is one of the main causes cannot be considered by the previous simplified theoretical model, so another theoretical model is introduced.

Korea Advanced Institute of Science and Technology (KAIST), Mechanical Engineering, 291 Daehak-ro, Yuseong-gu, Daejeon 34141, Republic of Korea. email: yjpark@kaist.ac.kr

**Methods**

**The circular active noise barrier and the theoretical model.** The circular active noise barrier is briefly described. The structure is shown in Fig. 1. A control filter for ANC is obtained to minimize the acoustic potential energy of the target control space as shown in Eq. (1).

$$C_w = \int_V \frac{|P_n - K_w P_c|^2}{2\rho c^2} dv \tag{1}$$

Here,  $P_n [Pa]$  and  $P_c [Pa]$  are respectively the pressure over the target control space by noise and the control source.  $V$  is the target control space, and  $S$  is the cross-section of the axis-symmetric structure.  $\rho [kg/m^3]$  and  $c [m/s]$  are the air density and speed of sound, respectively. The obtained control filter  $K_w$  to minimize Eq. (1) is provided in Eq. (2).

$$K_{w,opt} = \left[ \int_V P_c P_n dv \right] \left[ \int_V P_c P_c dv \right]^{-1} \tag{2}$$

Because of the axisymmetric structure, the integral calculation domain for calculating the control filter can be changed from space to surface.

$$K_{w,opt} = \left[ \int_S P_c P_n r ds \right] \left[ \int_S P_c P_c r ds \right]^{-1} \tag{3}$$

The residual acoustic potential energy is given in Eq. (4).

$$C_e = \int_V \frac{|P_n - K_{w,opt} P_c|^2}{2\rho c^2} dv \tag{4}$$

Noise reduction is defined as the reduction of the acoustic potential energy in the target control space as shown in Eq. (5).

$$NR = 10 \log_{10} \frac{C_0}{C_e} \tag{5}$$

$C_0$  is the acoustic potential energy in the target control space before reducing the noise ( $C_0 = \int_V \frac{|P_n|^2}{2\rho c^2} dv$ ).

Noise reduction performance in the frequency band of interest is defined as delineated in Eq. (6).

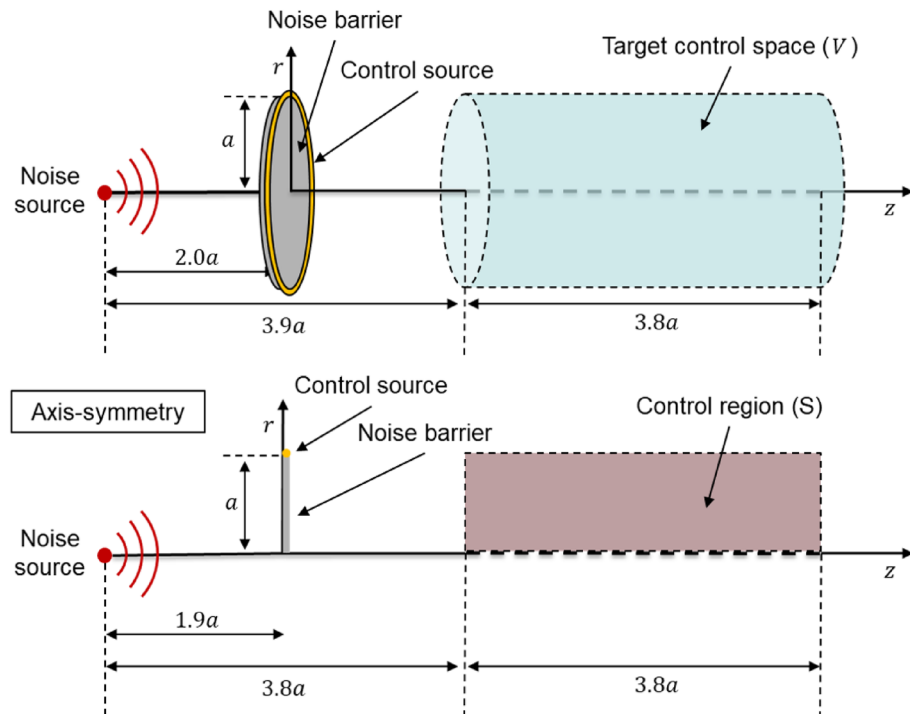


**Figure 1.** Configuration of the circular active noise barrier (top) and illustration of an axisymmetric structure in two-dimension (bottom). The control source is a circular line source in the prior study.  $a$  is the radius of the barrier.  $V$  is the target control space, and  $S$  is the cross-section of the axis-symmetric structure.

$$NR_{performance} = 10 \log_{10} \frac{C_{int,0}}{C_{int,e}} \quad (6)$$

$C_{int,0}$  is the summation of the  $C_0$  in the frequency band of interest ( $C_{int,0} = \int_F C_0 df$ ).  $C_{int,e}$  is the summation of the  $C_e$  in the frequency band of interest ( $C_{int,e} = \int_F C_e df$ ).  $F$  is the frequency band of interest.

In order to obtain the control filter in Eq. (3), the theoretically calculated pressure is used. In the case of the noise, the equation established by Flammer<sup>16</sup> is used by assuming the circular barrier as a very thin disk under an acoustically hard condition. The equation is written in the oblate spheroidal coordinate. The relations between the Cartesian coordinate  $(x, y, z)$  and the oblate spheroidal coordinate  $(\xi, \eta, \phi)$  are given in Eq. (7).

$$\begin{aligned} x &= a\sqrt{(1-\eta^2)(\xi^2+1)}\cos(\phi) \\ y &= a\sqrt{(1-\eta^2)(\xi^2+1)}\sin(\phi) \\ z &= a\eta\xi \end{aligned} \quad (7)$$

Here,  $a$  is the radius of a circular barrier. The pressure of noise located at  $(\eta_0, \xi_0, \phi_0)$  with an acoustically hard circular barrier at the origin is shown in Eq. (8). The harmonic term ( $e^{i\omega t}$ ) is omitted.

$$\begin{aligned} p_{noise}(\eta, \xi, \phi) &= \frac{ik}{2\pi} \sum_{m=0}^{\infty} \sum_{n=m}^{\infty} \frac{\varepsilon_m}{N_{mn}(-ika)} S_{mn}(-ika, \eta_0) S_{mn}(-ika, \eta) \cos(m(\phi - \phi_0)) \\ &\times \left[ R_{mn}^{(1)}(-ika, i\xi_{<}) R_{mn}^{(3)}(-ika, i\xi_{>}) - \frac{R_{mn}^{(1)' }(-ika, 0)}{R_{mn}^{(3)' }(-ika, 0)} R_{mn}^{(3)}(-ika, i\xi) R_{mn}^{(3)}(-ika, i\xi_0) \right] \end{aligned} \quad (8)$$

Here,  $N_{mn}$  is the normalization constant and  $\varepsilon_m$  is 1 for  $m = 0$  and 2 for all other values.  $k = \frac{2\pi}{\lambda}$  is wavenumber.  $\xi_{<}$  is  $\min(\xi, \xi_0)$  and  $\xi_{>}$  is  $\max(\xi, \xi_0)$ .  $S_{mn}(-ika, \eta)$  is the oblate spheroidal angular wave function and  $R_{mn}^{(j)}(-ika, i\xi)$  is the oblate spheroidal radial wave function of the  $j^{\text{th}}$  kind.

In the case of the control source, a circular control source is used in the prior study<sup>13</sup>. However, a circular control source which is an infinitely distributed monopole sources in a circle cannot consider the interaction between the control speakers and the barrier. The reason why control speakers are placed at the edge of the barrier is different from a circular source is illustrated in Fig. 2.

As shown in Fig. 2, a speaker in the free field can be assumed as a monopole when a speaker is much smaller than the wavelength. However, a speaker attached to the edge of the barrier generates a different sound field compared with a monopole source because some of the sound propagating to the rear of the speaker is blocked by the barrier. To address this, an oscillating ring in a finite closed-back baffle is introduced to serve as a control source for considering the interaction between the speaker and the barrier. It is in a finite baffle with a closed-back, and the ring vibrates to generate sound, as shown in Fig. 3. The ring thickness ( $r_o-r_i$ ) is determined by the diameter of the diaphragm of the control speaker.

Due to the structure of the vibrating piston with the internal baffle, an effect similar to the interaction between the speaker and the barrier appears, and therefore the case where the control speakers are placed on the edge of a circular barrier can be approximated. The equation of the oscillating ring in a finite closed-back baffle can be derived by changing the boundary condition of the oscillating disk in a closed-back baffle<sup>17</sup>. Compared to the circular control source, the model becomes more complex, but the axisymmetric property is maintained.

## Results

**Noise reduction performance in the simulation.** The noise reduction performance of the proposed hybrid noise control system is checked through a FEM simulation by Comsol. In the simulation, the material of the barrier is selected as aluminum, and six simple speaker models are arranged on the edge of the barrier. The simple speaker model used in the simulation is shown in Fig. 4. It is a closed-enclosure structure, and the inside is filled with air. The sound is generated by setting the velocity of the diaphragm.

The speakers are placed so that the center of the speaker is on the edge of the barrier. The configuration of the simulation model is illustrated in Fig. 5.

The insertion loss on the  $r-z$  plane is shown in Fig. 6 to confirm whether the noise is reduced in the control space. The insertion loss is defined as Eq. (9).  $P_{n,0}$  is the pressure when the noise reduction methods are not applied, and  $P_e$  is the residual pressure reduced by using the circular active barrier.  $k = \frac{2\pi}{\lambda}$  is the wavenumber.

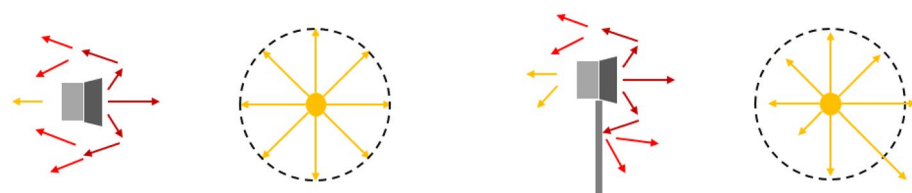


**Figure 2.** Configuration of the generated sound by a speaker in the free field (left) and a speaker with a barrier (right).

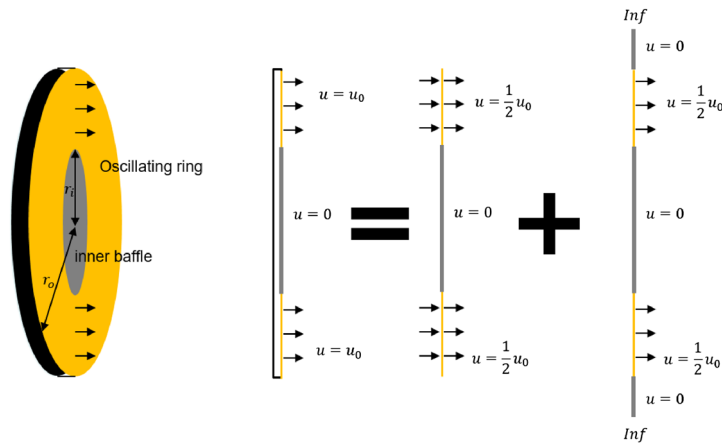


**Figure 3.** Configuration of an oscillating ring in a finite closed back baffle to consider the interaction between the speaker and the barrier.

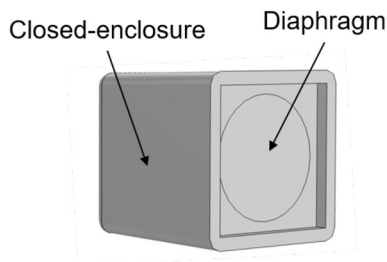


**Figure 4.** The speaker model used in the simulation is a closed-enclosure structure, and the sound is generated by oscillating the diaphragm.

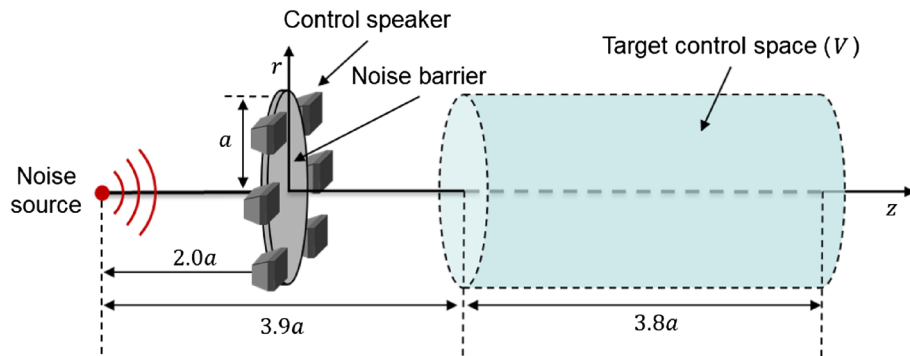


**Figure 5.** Configuration of the simulation model. A simple speaker model is used for control sources.  $a$  is the radius of the barrier.  $V$  is the target control space.

$$Insertionloss : 10 \log_{10} \left[ \frac{P_{n,0}}{P_e} \right]^2 \quad (9)$$

It is shown that the noise around the control space is reduced. Noise in a space opposite the control space may increase due to the control sound field for noise reduction in the target control space. If it is required to prevent the increase in noise over the space where the noise source is located, using a unidirectional control speaker can be one solution.

The noise reduction defined in Eq. (5) is shown in Fig. 7. Theoretical model 1 is the case of using a circular source as a control source, and the proposed theoretical model 2 uses the oscillating ring in a finite closed-back baffle as a control source.

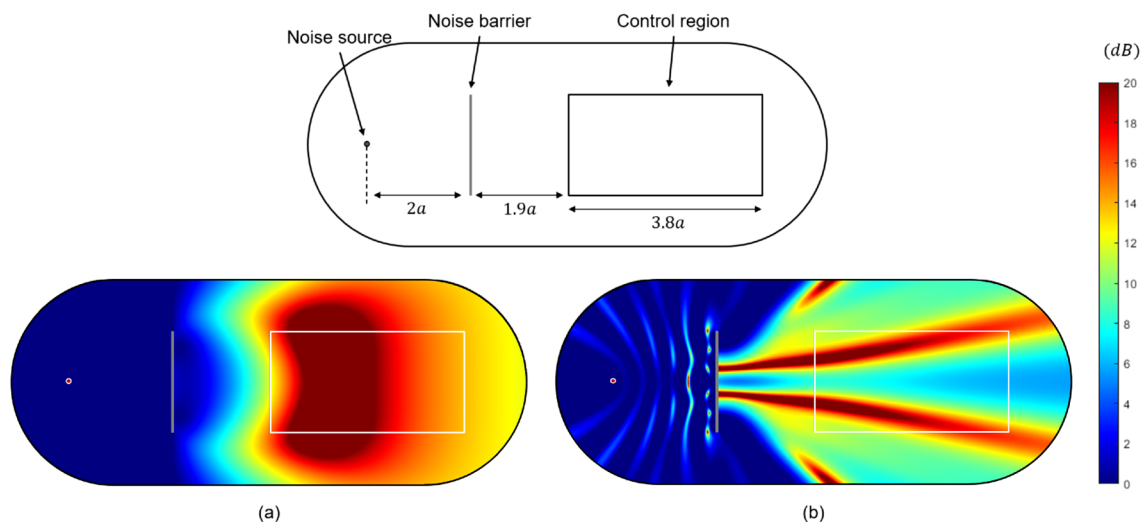


**Figure 6.** The cross-section of the simulation model on the  $r - z$  plane (top). Insertion loss on the  $r - z$  plane: (a)  $ka = 0.95$  and (b)  $ka = 9.5$ .

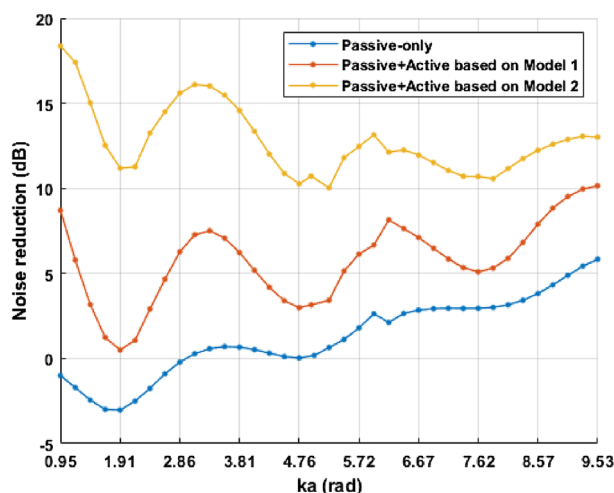


**Figure 7.** Noise reduction of circular barrier (blue), circular active noise barrier using the control filter obtained through the circular control source (red), and circular active noise barrier using the proposed theoretical model-based control filter (yellow).

It is shown that the circular active noise barrier can reduce noise in the wide frequency band. However, it is shown that there is a performance gap between the two cases where different theoretical model-based control filters are used. The control filter based on the oscillating ring in a finite closed-back baffle model achieves better noise reduction than the control filter obtained by using a circular control source due to the interaction between the speaker and the barrier. As a result, the validity of the oscillating ring in a finite closed-back baffle as a control source in the theoretical model of the circular active noise barrier is confirmed.

**Experiments.** *Experimental set-up.* The barrier was made of aluminum with a thickness of 6 mm and a density of  $2.7\text{ g/cm}^3$ . The radius of the barrier is 0.26 m. The speakers are placed so that the center of the speaker is on the edge of the barrier. The experiment was conducted in an anechoic chamber with a width and length of 3.6 m, a height of 2.4 m, and a minimum allowable frequency of 100 Hz. As noise and control sources, commercial speakers capable of generating a 200 to 20 kHz band were used. In the case of the frequency band of interest, the band from 200 Hz, the lowest frequency that the speaker can generate, to 2000 Hz, where the noise barrier can achieve noise reduction of 5 dB or more, is determined. Measurements were performed at intervals of 10 cm in one section of the target control space. The sampling frequency is 6000 Hz and Gaussian white noise was used as the noise signal. Open loop ANC is conducted without error microphones using the theoretically calculated control filter. In the case of the control filter, the time domain control filter obtained by inverse Fourier transform of the control filter in the frequency domain was used. The constructed experimental system is shown in Fig. 8. The globe experimental setup is the same as the previous study<sup>13</sup>.

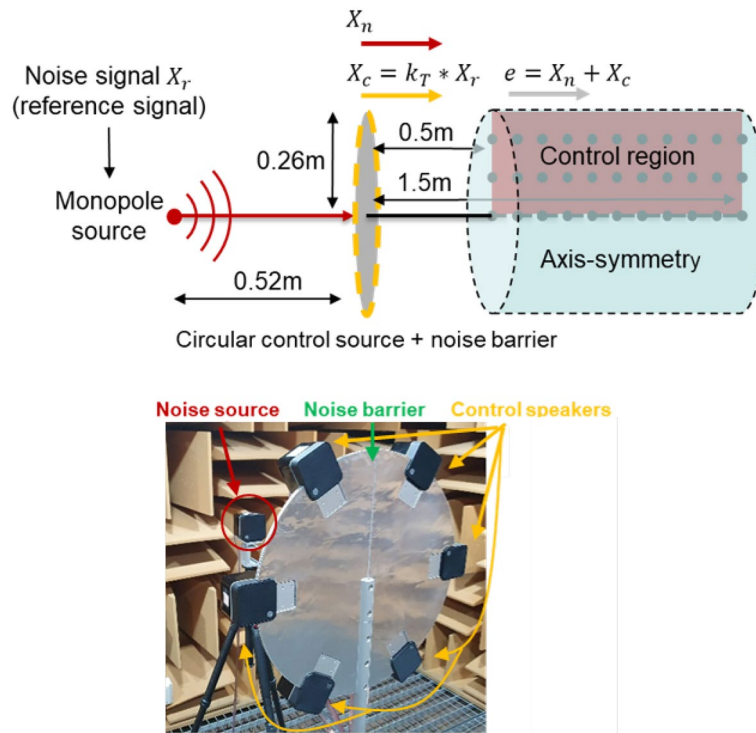


**Figure 8.** Configuration of the experimental system (top) and the constructed experimental system in an anechoic chamber (bottom).

*Experiment results.* The measured noise reduction as defined in Eq. (5) is shown in Fig. 9. Theoretical model 1 is the case of using a circular source as a control source, and the proposed theoretical model 2 uses the oscillating ring in a finite closed-back baffle.

Similar to the simulation results, the circular noise barrier attenuates noise by about 5dB or more above 2000Hz, but it is shown that the noise reduction is insignificant or the noise is amplified below 1000Hz. In the hybrid noise control system, performance is improved by applying ANC. However, in the case of model 1, a difference in the control sound field occurs due to the interaction between the speakers and the barrier, resulting in poor performance. Otherwise, in the case of model 2, the hybrid noise control system achieves a noise reduction of about 10.6dB in the frequency band of interest by using the theoretically calculated control filter. The noise

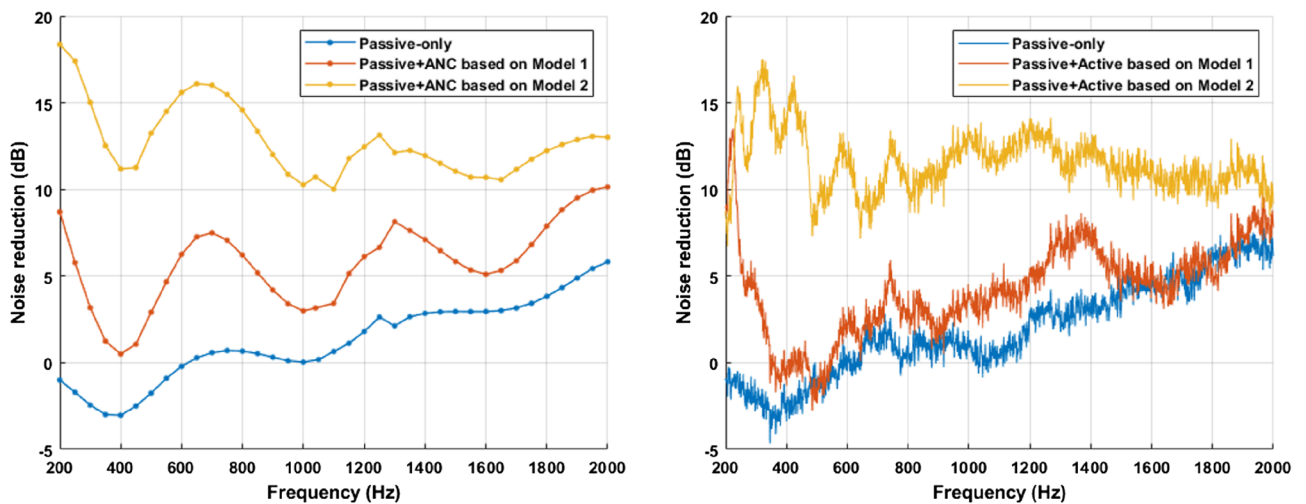


**Figure 9.** Noise reduction performance in the simulation (left) and in the experiment (right): noise barrier (blue), hybrid noise control using the control filter based on model 1 (red), and hybrid noise control using the control filter based on model 2 (yellow).

	Noise reduction performance
Circular barrier	1.3 dB
Hybrid noise control (model 1)	3.6 dB
Hybrid noise control (model 2)	10.6 dB

**Table 1.** Noise reduction performance in the experiment.

reduction performance as defined in Eq. (6) is shown in Table 1. As a result, it is validated that the oscillating ring in a finite closed-back baffle is more appropriate for the circular active noise barrier than a circular source.

## Discussion

According to the results in Fig. 9, it is shown that when model 1 is applied, the worse performance is achieved compared to the previous results<sup>13</sup>. The reason is that the placement position of the control speaker is moved inside for better performance. In an actual system, noise is scattered due to the arranged control speakers. However, the volume of the control speaker is not considered when theoretically calculating the sound field of noise, so the performance is degraded due to the difference in the sound field of noise. In order to reduce the effect of the volume of the control speaker, in this study, the speakers are placed so that the center of the speaker is on the edge of the barrier as shown in Fig. 10. Since the control speakers are moved inside the barrier, the interaction between the speakers and barrier becomes more significant. Therefore, when model 1 including a circular control source is applied, worse performance is achieved.

For maximum performance of the constructed experimental system, the FIR Wiener filter solution<sup>18</sup> obtained by the measured data over the target control space is used. The measured noise reduction as defined in Eq. (5) is shown in Fig. 11. The noise reduction performance as defined in Eq. (6) is 12.8 dB, constituting a difference in the performance of about 2.2 dB compared to the case of applying the theoretical model-based control filter.

The noise reduction by using the theoretical control filter is lower than the case of the Wiener filter solution in a range of 450–900 Hz. A noticeable difference in the secondary path below 1000 Hz occurs between the theoretical model and the experimental system as shown in Fig. 12.

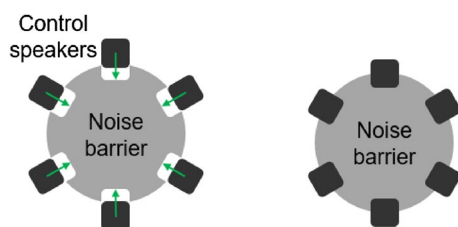


**Figure 10.** Configuration of the position of the control speakers.

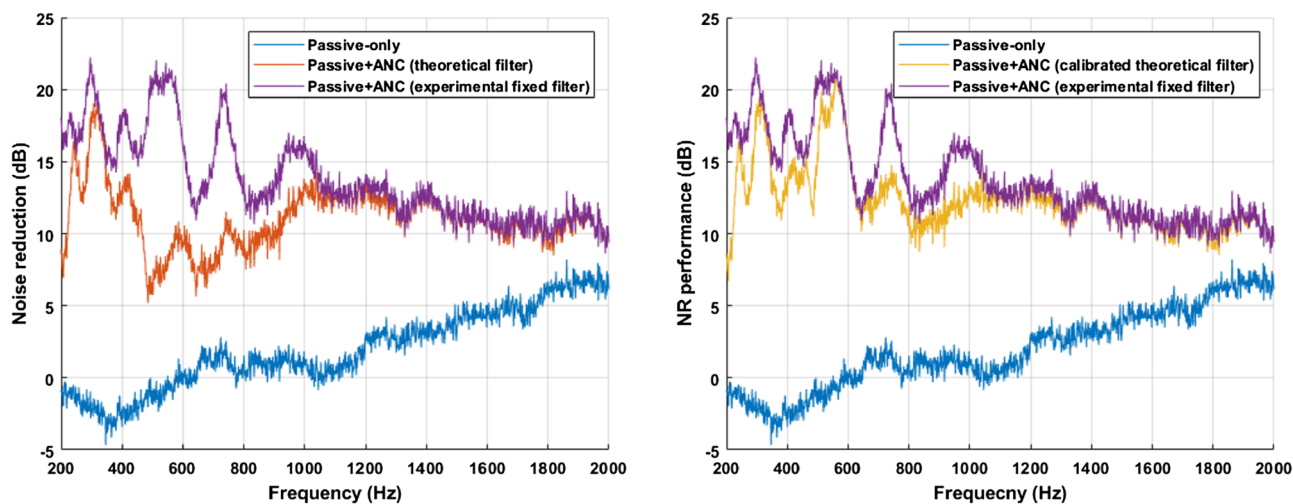


**Figure 11.** Noise reduction in the experiment: through the barrier only (blue), circular active noise barrier based on model 2 (red), circular active noise barrier using the calibrated theoretical control filter based on the preliminary experiment (yellow), and circular active noise barrier using the Wiener filter solution (purple).

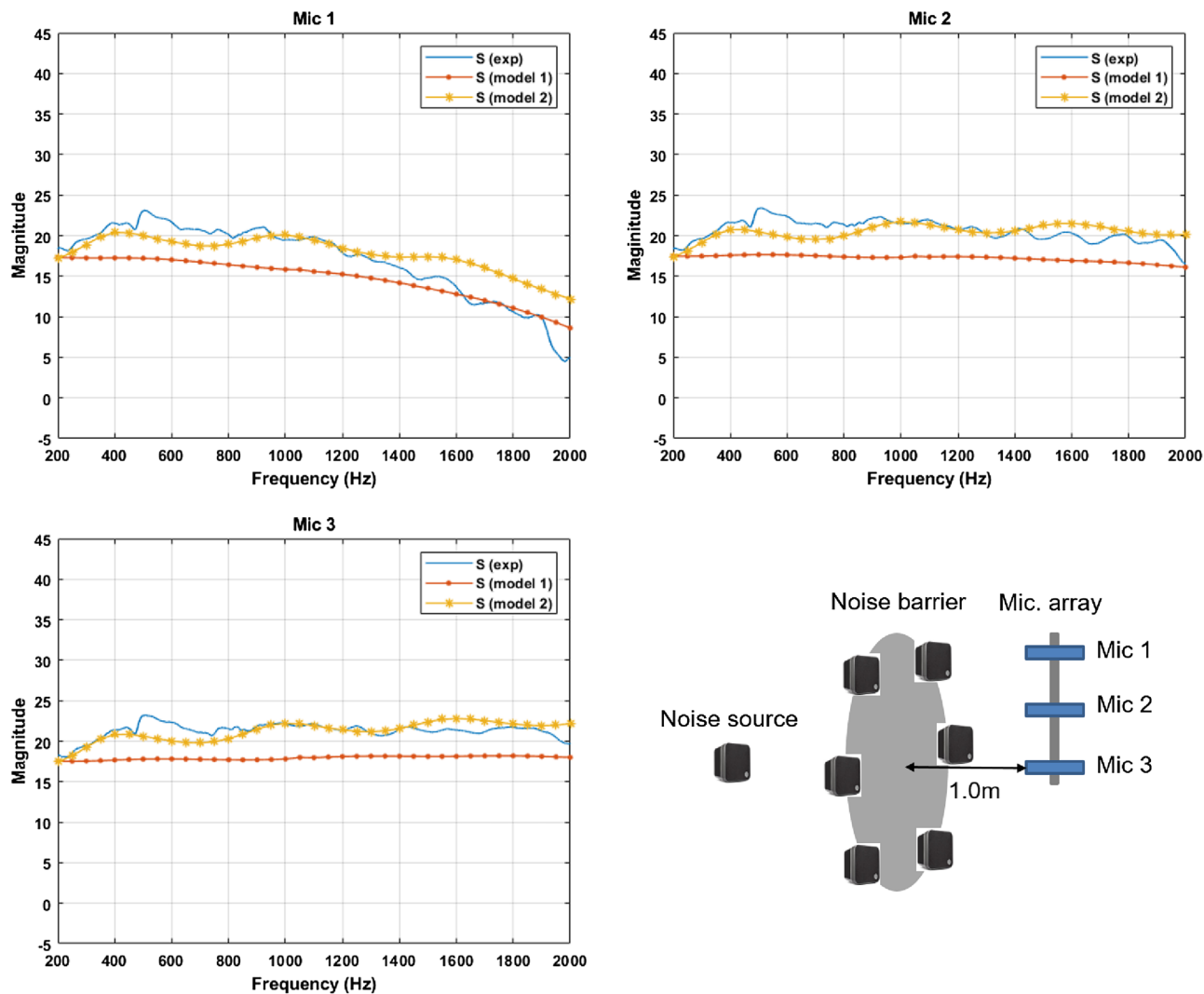


**Figure 12.** The secondary path at a distance of 1 m from the barrier: in the experiment (blue), model 1 (red), model 2 (yellow).

For performance improvement, the theoretical filter should be calibrated to consider the system dynamics, which are not included in the theoretical model. Noise reduction is shown in Fig. 11 when calibration based on the preliminary experiment in the anechoic chamber is applied. It is shown that the performance approaches that of the case of the Wiener filter solution.

## Conclusions

A circular active noise barrier that considers the interaction between a speaker array and a barrier is proposed to improve the noise reduction performance. In order to reduce the scattering of the noise due to the control speakers, the position of the control speaker is moved inside the barrier. This causes the influence of the interaction between the control speakers and a barrier to become more significant. Therefore, the oscillating ring in a finite closed-back baffle is introduced for the control source and the improvement of the noise reduction performance is validated through a simulation and experiment. It is confirmed that noise reduction similar to the experimental maximum performance could be achieved by using the theoretical control filter when the control filter is tuned based on a preliminary experiment. Further research such as studying methods of obtaining the required information for ANC or the means of updating the control filter should be carried out.

## Data availability

The datasets generated and analyzed during the current study are available from the corresponding author on reasonable request.

Received: 5 August 2022; Accepted: 6 January 2023

Published online: 14 February 2023



## References

1. World report on hearing. *Geneva: World Health Organization*. Licence: CC BY-NC-SA 3.0 IGO (2021)
2. Ise, S., Yano, H. & Tachibana, H. Basic study on active noise barrier. *J. Acoust. Soc. Jpn.* **12**, 299–306. <https://doi.org/10.1250/ast.12.299> (1991).
3. Wang, T. *et al.* Research on active noise control method compensating for acoustic metamaterial noise barrier in transformer noise reduction. In *2018 IEEE 2nd International Electrical and Energy Conference (CIEEC)* 648–652, <https://doi.org/10.1109/CIEEC.2018.8745747> (2018).
4. Lee, H. M., Wang, Z., Lim, K. M. & Lee, H. P. Review of active noise control applications on noise barrier in threedimensional/open space: myths and challenges. *Fluct. Noise Lett.* **18**, 1–21. <https://doi.org/10.1142/S0219477519300027> (2019).
5. Sohrabi, S., Gómez, T. P. & Garbí, J. R. Suitability of active noise barriers for construction sites. *Appl. Sci.* <https://doi.org/10.3390/app10186160> (2020).
6. Lam, B., Gan, W.-S., Shi, D., Nishimura, M. & Elliott, S. Ten. questions concerning active noise control in the built environment. *Build. Environ.* <https://doi.org/10.3390/app10186160> (2021).
7. Kuo, S. & Morgan, D. *Active Noise Control Systems: Algorithms and dsp Implementations* (John Wiley and Sons Inc, 1955).
8. Omoto, A. & Fujiwara, K. A study of an actively controlled noise barrier. *J. Acoust. Soc. Am.* **94**, 2173–2180. <https://doi.org/10.1121/1.407488> (1993).
9. Sohrabi, S., Gómez, T. P. & Garbí, J. R. Proper location of the transducers for an active noise barrier. *J. Vib. Control* <https://doi.org/10.1177/10775463221077490> (2022).
10. Berkhoff, A. P. Control strategies for active noise barriers using near-field error sensing. *J. Acoust. Soc. Am.* **118**, 1469–1479. <https://doi.org/10.1121/1.1992787> (2005).
11. Hart, C. R. & Lau, S.-K. Active noise control with linear control source and sensor arrays for a noise barrier. *J. Sound Vib.* **334**, 15–26. <https://doi.org/10.1016/j.jsv.2011.08.016> (2012).
12. Chen, W., Rao, W., Min, H. & Qiu, X. An active noise barrier with unidirectional secondary sources. *Appl. Acoust.* **72**, 969–974. <https://doi.org/10.1016/j.apacoust.2011.06.006> (2011).
13. Lee, S. & Park, Y. Compact hybrid noise control system: Anc system equipped with circular noise barrier using theoretically calculated control filter. *Appl. Acoust.* **188**, 108472. <https://doi.org/10.1016/j.apacoust.2021.108472> (2022).
14. Lee, S. & Park, Y. Noise reduction performance of active noise control with barrier using theoretical control filter. In *The 15th International Conference on Motion and Vibration Control (MoViC 2020)* 10022, <https://doi.org/10.1299/jsmaintmovic.2020.15.10022> (2020).
15. Lee, S. & Park, Y. Performance degradation factors of compact hybrid noise control system using theoretical control filter. In *The 19th Asia Pacific Vibration Conference (2021 APVC)* (2022).
16. Flammer, C. *Spheroidal Wave Functions* (Stanford University Press, 1957).
17. Mellow, T. & Kärkkäinen, L. On the sound field of an oscillating disk in a finite open and closed circular baffle. *J. Acoust. Soc. Am.* **118**, 1311–1325. <https://doi.org/10.1121/1.2000828> (2005).
18. Hayes, M. H. *Statistical Digital Signal Processing and Modeling* (John Wiley and Sons Inc, 1996).

## Acknowledgements

This work was supported by a National Research Foundation of Korea (NRF) Grant funded by the Korean government (MSIT) (No. NRF-2020R1A2C1012904).

## Author contributions

S.H.L. conducted the simulation and experiment. All authors analyzed the results and reviewed the manuscript.

## Competing interests

The authors declare no competing interests.

## Additional information

**Correspondence** and requests for materials should be addressed to Y.P.

**Reprints and permissions information** is available at [www.nature.com/reprints](http://www.nature.com/reprints).

**Publisher's note** Springer Nature remains neutral with regard to jurisdictional claims in published maps and institutional affiliations.



**Open Access** This article is licensed under a Creative Commons Attribution 4.0 International License, which permits use, sharing, adaptation, distribution and reproduction in any medium or format, as long as you give appropriate credit to the original author(s) and the source, provide a link to the Creative Commons licence, and indicate if changes were made. The images or other third party material in this article are included in the article's Creative Commons licence, unless indicated otherwise in a credit line to the material. If material is not included in the article's Creative Commons licence and your intended use is not permitted by statutory regulation or exceeds the permitted use, you will need to obtain permission directly from the copyright holder. To view a copy of this licence, visit <http://creativecommons.org/licenses/by/4.0/>.

© The Author(s) 2023